Clathrin-independent Pinocytosis Is Induced in Cells Overexpressing a Temperature-sensitive Mutant of Dynamin

Hanna Damke,* Takeshi Baba,* Alexander M. van der Bliek,‡ and Sandra L. Schmid*

*Department of Cell Biology, The Scripps Research Institute, La Jolla, California 92037; and ‡Department of Biological Chemistry, University of California, Los Angeles, California 90024

Abstract. A stable HeLa cell line expressing a dynamin mutant, dyn^{ts}, exhibits a temperature-sensitive defect in endocytic clathrin-coated vesicle formation. Dyn^{ts} carries a point mutation, G273D, corresponding to the *Drosophila shibire^{ts1}* allele. The ts-defect in receptor-mediated endocytosis shows a rapid onset (<5 min) and is readily reversible. At the nonpermissive temperature (38°C) HRP uptake is only partially inhibited. Moreover, when cells are held at the nonpermissive temperature, fluid phase uptake fully recovers to wild-type levels within 30 min, while receptor-mediated endocytosis remains inhibited. The residual HRP uptake early after shift to the nonpermissive temperature and the induced HRP uptake that occurs after recovery are insensitive to cytosol acidification under conditions that potently inhibit receptor-mediated endocytosis of Tfn. Together, these results suggest that a dynamin- and clathrin-independent mechanism contributes to the total constitutive pinocytosis in HeLa cells and that dyn^{ts} cells rapidly and completely compensate for the loss of clathrin-dependent endocytosis by inducing an alternate endocytic pathway.

DYNAMIN is a 100-kD GTPase originally isolated as a nucleotide-dependent microtubule binding protein (Shpetner and Vallee, 1989). Dynamin function in vivo has been studied using transiently (Herskovits et al., 1993; van der Bliek et al., 1993) and stably (Damke et al., 1994) transfected cells overexpressing dominant interfering, GTPase-defective mutants. Receptor-mediated endocytosis is potently and specifically inhibited in stably transformed cells with inducible expression of a dynamin mutant (designated K44A and previously referred to as ele1) defective in GTP binding (Damke et al., 1994). Phenotypic characterization of these cells established that dynamin function is required for the formation of constricted coated pits at the plasma membrane. Importantly, no other vesicular trafficking events, including protein transport through the exocytic pathway, receptor recycling through the endosomal pathway or clathrin-coated vesicle-mediated sorting of lysosomal hydrolases were affected (Damke et al., 1994). Consistent with this specificity of function and even when overexpressed >20-fold, membrane-associated dynamin is exclusively localized to clathrin-coated pits on the plasma membrane (Damke et al., 1994). These membrane binding sites are apparently saturable since in cells overexpressing dynamin, much of the excess is present in the cytosolic pool.

These studies established the specificity of dynamin function in vivo. However, prolonged incubation times (24–48 h) were required to allow sufficient accumulation of mutant dynamin to functionally overwhelm endogenous dynamin. Therefore, we were unable to establish that dynamin was directly required for coated vesicle budding in mammalian cells. Genetic evidence for a direct role of dynamin in endocytosis comes from phenotypic analysis of the temperature-sensitive (ts) *shibire* mutant of *Drosophila*. The *shibire* gene encodes a protein that is 70% identical to mammalian dynamin (van der Bliek and Meyerowitz, 1991; Chen et al., 1991). Within a minute after shifting *shibire^{ts}* flies to the nonpermissive temperature, endocytosis is blocked and coated pits accumulate at the plasma membrane in all tissues examined (Poodry and Edgar, 1979; Kosaka and Ikeda, 1983*a*; Koenig and Ikeda, 1990; Tsuruhara et al., 1990). While only one isoform of dynamin has been detected in *Drosophila*, at least three isoforms of dynamin, each ~70% identical to *shibire* and >70% identical to each other have been detected in mammals. Dynamin-1, the originally identified protein, is exclusively expressed in neuronal cells (Nakata et al., 1991; van der Bliek et al., 1993; Sontag et al., 1994). Dynamin-2 is a ubiquitously expressed isoform (Cook et al., 1994; Sontag et al., 1994) that has also been localized to endocytic clathrin-coated pits (Damke et al., 1994) and appears to be functionally equivalent to dynamin-1. Dy-

Address correspondence to Sandra L. Schmid, Department of Cell Biology, The Scripps Research Institute, 10666 N. Torrey Pines Rd., La Jolla, CA 92037. Tel.: (619) 554-2311. Fax: (619) 554-6253. E-mail: slschmid@scripps.edu.

Dr. Baba's current address is Department of Anatomy, Yamanashi Medical University, Yamanashi 409-38, Japan.

This is manuscript number 9220-CB from The Scripps Research Institute.

namin-3 is a testes specific isoform of unknown function (Nakata et al., 1993). Whether these other dynamin isoforms are functionally distinct from the single *shibire* gene product is not known.

Fluid phase pinocytosis is blocked in *shibire* cells (Kosaka and Ikeda, 1983*a*; Tsuruhara et al., 1990) suggesting that the *shibire* protein is required for all pinocytic events. While only coated invaginations are seen to accumulate in nonneuronal tissues (Kosaka and Ikeda, 1983*a*), both coated and noncoated invaginations accumulate on presynaptic membranes at the nonpermissive temperature (Kosaka and Ikeda, 1983*b*). In contrast, fluid phase endocytosis proceeds normally in mammalian cells overexpressing dynamin-1 mutants (Herskovits et al., 1993; Damke et al., 1994), indicating the existence of a dynamin-independent and most likely clathrin-independent pinocytic pathway. While it is clear that fluid phase pinocytosis can occur in mammalian cells under conditions that inhibit clathrin-dependent endocytosis (Sandvig et al., 1987), the existence and function of a constitutive clathrin-independent endocytic pathway remains controversial (Hansen et al., 1991; Watts and Marsh, 1992). For example, we (Damke et al., 1994) and others (Watts and Marsh, 1992; Cupers et al., 1994) have argued that clathrin-independent mechanisms of pinocytosis can be induced in response to perturbations in clathrin-dependent endocytosis. Thus, the existence of a constitutive clathrin-independent pinocytic mechanism and the potential role of mammalian dynamin in this process remain unresolved.

To address these issues, a point mutation (G273D) was introduced into human dynamin-1 to generate a mutant, designated dyn^{ts}, that is homologous to the *shibire*^{ts1} protein. Stable HeLa cell transformants expressing dyn^{ts} in a tetracycline-responsive manner were established. Here we show that these dyn^{ts} cells, like their *shibire* counterparts, exhibit a rapid, reversible and temperature-sensitive block in receptor-mediated endocytosis. Furthermore, we show that a dynamin-independent pinocytic process, accounting for ~30% of constitutive fluid phase uptake, continues after the temperature shift and that this pathway is induced within 30 min to fully restore fluid phase uptake to wild-type levels. The fluid phase pinocytosis that occurs at both early and late times after shift to the nonpermissive temperature is insensitive to cytosol acidification, a condition that selectively perturbs clathrin-dependent endocytosis (Sandvig et al., 1987; Cupers et al., 1994). These results suggest that a clathrin and dynamin-independent pinocytic pathway is induced in dyn^{ts} cells to rapidly compensate for the loss of the clathrin-dependent contribution to bulk endocytosis.

Materials and Methods

Reagents

The monoclonal anti-hemagglutinin antibody, 12CA5, was provided by I. A. Wilson (The Scripps Research Institute, La Jolla, CA). Mouse monoclonal anti-dynamin antibodies, hudy-1 and hudy-3, were prepared against recombinant human dynamin-1 as described (Warnock et al., 1995). Primary monoclonal antibodies were purified by affinity chromatography on protein G–Sepharose (Pierce Chemicals, Rockford, IL). Texas Red-conjugated secondary antibody, Texas Red-conjugated transferrin and rhodamine phalloidin were purchased from Molecular Probes (Eugene, OR).

Human diferric transferrin (Tfn)[1] was from Boehringer-Mannheim (Indianapolis, IN). Tfn was biotinylated as previously described (Smythe et al., 1992). Cytochalasin D, pronase and [4-(2-aminoethyl)-benzenesulfonylfluoride, HCl] (AEBSF) were from Calbiochem Novabiochem (La Jolla, CA). 5-[N,N-Hexamethylene]-amiloride and reagent-grade chemicals were obtained from Sigma Chem. Co. (St. Louis, MO) or Boehringer Mannheim unless otherwise specified.

Preparation of cDNA Constructs

A temperature-sensitive mutant of human dynamin, designated dyn^{ts}, was generated by site-directed mutagenesis of the glycine at position 273 to aspartic acid corresponding to the known point mutation in the *shibire*^{ts1} allele (van der Bliek and Meyerowitz, 1991). Dyn^{ts} was introduced into the pTM1-dyn^{wt} constructs using two different PCRs with Pfu polymerase (Stratagene Inc., La Jolla, CA) as previously described (van der Bliek et al., 1993). The cDNA was then modified by adding a linker fragment to the 5′ end of the coding sequence for fusion to the sequence, MEYDVPDYAH, containing an hemagglutinin (HA) epitope, as described in Damke et al., 1994. Subsequently the verified cDNA for the dyn^{ts} mutant was subcloned from the modified vaccinia expression constructs pTM1-HA-dyn^{ts} into the tetracycline-inducible expression plasmid pUHD10-3 as described (Damke et al., 1994).

Generation of Stably Transformed Mutant Cell Lines

The stable HeLa cell line tTA-HeLa, expressing the chimeric tetracycline regulatable transcription activator was kindly provided by H. Bujard (ZMBH, Heidelberg, FRG). Cells were maintained in DME supplemented with 10% (vol/vol) FBS, 100 U/ml each of penicillin and streptomycin and 400 μg/ml active G418 (Geneticin; GIBCO BRL, Gaithersburg, MD). The construct pUHD10-3 encoding HA-tagged dynamin^{ts} was used for the generation of stably transformed tTA-HeLa cells with tightly regulated expression of dynamin as described in Damke et al. (1995).

Cell Culture Conditions for tTA HeLa Cells Stably Transformed with the Dynamin cDNA

Cells were cultured at 37°C in DME, 10% FBS, 100 U/ml each of penicillin and streptomycin, 400 μg/ml G418 (selects for transactivator), 1–2 μg/ml tetracycline (suppresses dynamin expression), and 200 ng/ml puromycin to select for positive clones. Puromycin resistant clones were screened for their ability to express dynamin 48 h after induction in the absence of tetracycline at 37°C by SDS-PAGE and Western blot analysis.

For phenotypic analysis, subconfluent cultures were detached with trypsin/EDTA and ~1.2×10^6 cells were plated on 100-mm culture dishes in the presence (uninduced) or absence (induced) of tetracycline and incubated at the permissive temperature of 32°C at least 72 h before use. At this point the cells were ≤65% confluent. As dynamin expression and phenotype were highly dependent on the confluency of the cells it is important to use the cells at subconfluent density for biochemical and morphological analysis. This is also recommended for permanent culture of uninduced cells growing at 37°C. Inducible expression is also dependent on the passage number, and cells were therefore used at low passage number and routinely replaced by freshly thawed cells.

Western Blot Analysis

Cells were washed twice with PBS and detached with PBS, 5 mM EDTA. Cell pellets were immediately lysed in 1× Laemmli sample buffer and lysates were analyzed by SDS-PAGE on 7.5% gels and electroblotted to BA-S 83 nitrocellulose (Schleicher & Schuell, Inc., Keene, NH) by standard methods (Burnette, 1981). Nonspecific protein binding was blocked with 2% nonfat dry milk powder in Tris-buffered saline containing 0.1% Tween 20. The blots were incubated with the primary anti-dynamin antibody hudy-3 at 0.1 μg/ml, followed by detection with an alkaline phosphatase-conjugated secondary goat anti-mouse antibody (Pierce Chem. Co., Rockford, IL) and developed with an alkaline phosphatase color development kit (Bio-Rad, Hercules, CA).

1. *Abbreviations used in this paper*: BSST, biotinylated-transferrin; wt, wild-type; tet, tetracycline; Tfn, transferrin; Tfn-R, transferrin-receptor; HA, hemagglutinin; ts, temperature-sensitive.

Internalization Assays

Internalization assays using biotinylated-transferrin (BSST) were performed as previously described (van der Bliek et al., 1993). Cells induced at the permissive temperature were detached with PBS, 5 mM EDTA at RT for 5 min, briefly rinsed, and resuspended in PBS containing 1 mM $MgCl_2$, 1 mM $CaCl_2$, and 0.2% BSA, pH 7.4. The cell suspensions were then preshifted for various times at 30 or 38°C in waterbaths in which temperature was carefully adjusted using a digital thermometer. After the preshift, cells were rapidly cooled on ice and the ligand was added as a concentrated solution to a final concentration of 8 μg/ml BSST. The cell suspensions were then split into 50-μl aliquots (corresponding to 2×10^5 cells) for continuous internalization of BSST at 30 or 38°C for various times. Endocytosis was stopped by returning the samples to ice. Internalization of ligand was quantified after processing the samples for measuring avidin inaccessibility or MesNa resistance according to Carter et al. (1993).

Fluid Phase Uptake

Cells were grown on 35-mm plates for 72 h at 32°C (dyn^{K44A} cells for 48 h at 37°C) in the absence of tetracycline, washed twice with PBS and incubated with 4 mg/ml HRP in DME/20 mM Hepes, 0.2% BSA, pH 7.4, for various times. The uptake was terminated by aspirating the medium and by six subsequent washes with PBS, 1 mM $MgCl_2$, 1 mM $CaCl_2$, 0.2% BSA, pH 7.4, for 5 min at 4°C (Marsh et al., 1987). After two additional rinses with PBS at 4°C the cells were detached with 0.1% pronase in PBS, pH 7.4, which also removed any HRP unspecifically bound to the cell surface. The cell suspensions were pelleted through a sucrose cushion (0.5 M in PBS, pH 7.4) for 5 min at 1,000 *g* in a microfuge at 4°C. The cells were solubilized in PBS, 0.5% Triton X-100, and aliquots were assayed for enzyme activity using *o*-phenylenediamine as a substrate or for protein concentration using the Micro-BCA assay (Pierce Chem. Co.).

Cytosol Acidification

For acidification of the cytosol, wild-type or mutant cells grown at the permissive temperature were rinsed two times with DME-H (DME containing 2 mM L-glutamine and 20 mM Hepes, without bicarbonate), incubated for 30 min in DME-H, 0.2% BSA, rinsed two times in DME-H, 0.2% BSA, pH 5.0 and then incubated in 10 mM acetic acid in DME-H, 0.2% BSA, pH 5.0. To prepare DME-H pH 5.0, 1 M acetic acid, pH 5.0 (adjusted with NaOH) was diluted 1:100 into DME-H (adjusted to pH 5.0 with HCl) as described (Hansen et al., 1993). Controls were incubated in DME-H, 0.2% BSA, pH 5.0 or pH 7.4. Depending on the time of preshift at the nonpermissive temperature all solutions were prewarmed to 30 or 38°C. Then the medium was aspirated and the cells were incubated for up to 60 min in DME-H, 0.2% BSA containing HRP (4 mg/ml) and supplemented with 5 mM glucose at 30 or 38°C. Subsequently cells were processed as described above. For transferrin internalization cells in suspension were incubated under identical conditions in the presence of 8 μg/ml BSST as ligand.

Indirect Immunofluorescence

Dynamin wild-type and dyn^{ts} mutant tTA HeLa cells were grown in the absence of tetracycline on glass coverslips for 72 h at 32°C to ~60% confluency. The cells were incubated with TexasRed-conjugated transferrin (50 μg/ml) in serum free medium (DME, 20 mM Hepes, 0.2% BSA) at 30 or 38°C for 10 min. Then the cells were fixed in 4% paraformaldehyde in 0.1 M phosphate buffer, pH 7.4, for 30 min at room temperature, permeabilized with 0.05% saponin in PBS for 10 min, and then blocked in 1% BSA, 5% normal goat serum, 0.01% saponin, 0.02% sodium azide in PBS for 60 min. The cells were incubated with anti-HA mAb 12CA5 (2 μg/ml) for 30 min, washed in PBS and incubated with BODIPY FL-conjugated goat anti-mouse IgG antibody (Molecular Probes, Inc., Eugene, OR) for 30 min. The coverslips were washed and mounted in Aqua-Poly/Mount (Polyscience, Warrington, PA), viewed under a fluorescent microscope (Axiophoto; Carl Zeiss, Inc., Thornwood, NY), and photographed with Kodak T-Max 400 films.

Electron Microscopy

Cells were grown on glass coverslips as described above and incubated in serum free medium containing HRP (4 mg/ml) at 30 or 38°C for 10 min. These cells were then washed, fixed in 2.5% glutaraldehyde, 0.1 M phosphate buffer, pH 7.4, for 30 min, and incubated with 0.02% diaminobendizine, 0.005% H_2O_2 (Damke et al., 1994). The cells were then fixed with 2% OsO_4 for 30 min and embedded in Epon. Alternatively, cells were incubated for 15 min at 38°C before fixation in glutaraldehyde and OsO_4 (Damke et al., 1994). The ultrathin sections were observed under an electron microscope (model CM10; Phillips Sci., Mahwah, NJ) at 80 kV. Quantitation of coated pit accumulation was performed by photographing individual cell profiles at low magnification (3,000×) to measure surface length and then counting the number of coated pits at high magnification (15,000×). At least ten cell profiles were counted for each condition.

Results

A Human Homologue to the $shibire^{ts1}$ Mutation in Dynamin

To gain further insight into dynamin's function in mammalian cells and to provide genetic evidence that it plays a direct role in coated vesicle budding, we generated a point mutation in human dynamin homologous to the *Drosophila* $shibire^{ts1}$ allele. The *shibire* gene product is 70% identical to human dynamin and single point mutations responsible for the temperature-sensitive phenotype have been identified (van der Bliek and Meyerowitz, 1991). The most potent allele, ts^1, has a glycine to aspartic acid mutation towards the COOH-terminal end of the ~300–amino acid GTPase domain. This residue is conserved in human dynamin and the corresponding G273D mutation, designated dyn^{ts}, was made by site-directed mutagenesis. The cDNA encoding dyn^{ts} with an NH_2-terminal HA-epitope tag was inserted into a tetracycline (tet)-responsive expression vector (pUHD10-3) and used to transform tTA-HeLa cells expressing a tet-regulatable chimeric transcription activator (Gossen and Bujard, 1992; Damke et al., 1995). Clonal cell lines showing tight regulation of dynamin expression by tetracycline were selected and amplified, as previously described (Damke et al., 1994, 1995). Western blot analysis (Fig. 1) shows the tet-regulatable expression of dynamin constructs in these stably transformed tTA-HeLa cells. In the presence of tetracycline the expression of neuronal dynamin is not detectable with the dynamin-1 specific monoclonal antibody, hudy-3. In the absence of tetracycline, dynamin expression was induced to >20-fold over endogenous dynamin-2 (Damke et al., 1994). Equal expression levels were obtained in cells expressing either wt or mutant dynamin and when cells were incubated for either 48 h at 37°C or for 72 h at 32°C.

HeLa Cells Expressing $Dynamin^{ts}$ Show a Temperature-sensitive Defect in Receptor-mediated Endocytosis

Initial attempts to detect an endocytosis defect in transiently transfected cells expressing dyn^{ts} using the vaccinia-

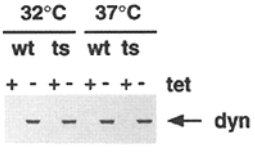

Figure 1. Western blot analysis with the anti-dynamin-1 mAb, hudy-3, demonstrates the tight control of tetracycline-regulatable expression of wild-type and ts-dynamin. The levels of protein accumulation were equivalent when cells were induced for 72 h at 32°C or for 48 h at 37°C. Lysates of equal numbers of cells were processed as described in Materials and Methods.

virus transfection system (van der Bliek et al., 1993) were unsuccessful (A. M. van der Blick, T. E. Redelmeier, and S. L. Schmid, unpublished data). Similarly, when tetracycline was removed to induce dyn^{ts} expression at 37°C, endocytosis was unaffected (data not shown) even though expression levels of recombinant dynamin were as high as for other mutants (Fig. 1). We reasoned that, since the mutation was predicted to be temperature-sensitive for function, it might be necessary to synthesize the mutant protein at the permissive temperature to generate a correctly folded and otherwise functional protein. Several temperatures were tested and we found that the optimum temperature for cell growth and induction of functional dyn^{ts} was 32°C. As can be seen in Fig. 1, 72 h after induction at 32°C dyn^{ts} accumulated in HeLa cells to high levels. When assayed at 30°C (the experimentally determined permissive temperature), endocytosis of transferrin (Tfn) in these cells was found to occur with the same rates and efficiencies as in cells expressing wt dynamin (Fig. 2 *A*). In contrast, when measured 15 min after shifting the cells to 38°C (the experimentally determined nonpermissive temperature) Tfn-internalization was severely inhibited in dyn^{ts} cells as compared to dyn^{wt} cells (Fig. 2 *B*). The extent of inhibition of the initial rate of Tfn uptake at the nonpermissive temperature in dyn^{ts} cells (81 ± 11%, n = 5) was similar to that previously reported (Damke et al., 1994) in cells expressing the dominant-interfering mutant, dyn^{K44A} (82 ± 8%, n = 10). Previous studies established that overexpression of wt dynamin had no effect on either the rate or extent of endocytosis (Damke et al., 1994).

Consistent with the *shibire* phenotype, cells expressing dyn^{ts} showed a rapid onset of the temperature-sensitive defect. The data in Fig. 3 *A* show that even without a preshift to the nonpermissive temperature, the amount of Tfn internalized after 10 min at 38°C was inhibited by ~45%. In fact, inhibition was apparent even at the earliest time (2.5 min) of Tfn internalization at 38°C (not shown). Maximal inhibition was obtained by 10–15 min after shift to the

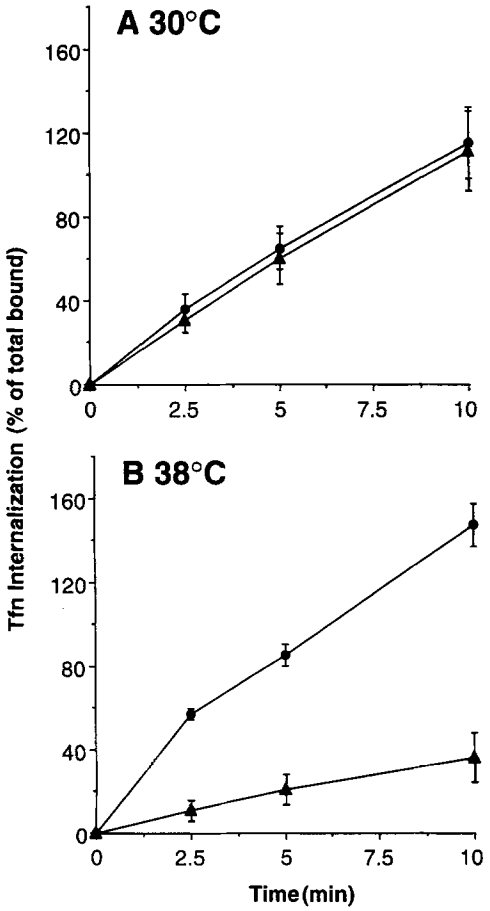

Figure 2. Receptor-mediated endocytosis of transferrin is inhibited in the dyn^{ts} mutant after shift to the nonpermissive temperature. After 72 h of induction in the absence of tetracycline at 32°C, the internalization of biotinylated transferrin was followed in cells expressing either wild-type dynamin (●) or the G273D, $dynamin^{ts}$ mutant (▲). Endocytosis was measured either at the permissive temperature of 30°C (*A*) or at the nonpermissive temperature of 38°C (*B*) after a 15 min preshift to 38°C. The amount of internalized BSST was determined by avidin inaccessibility as described in Materials and Methods. Results shown are the average ± SD on five experiments.

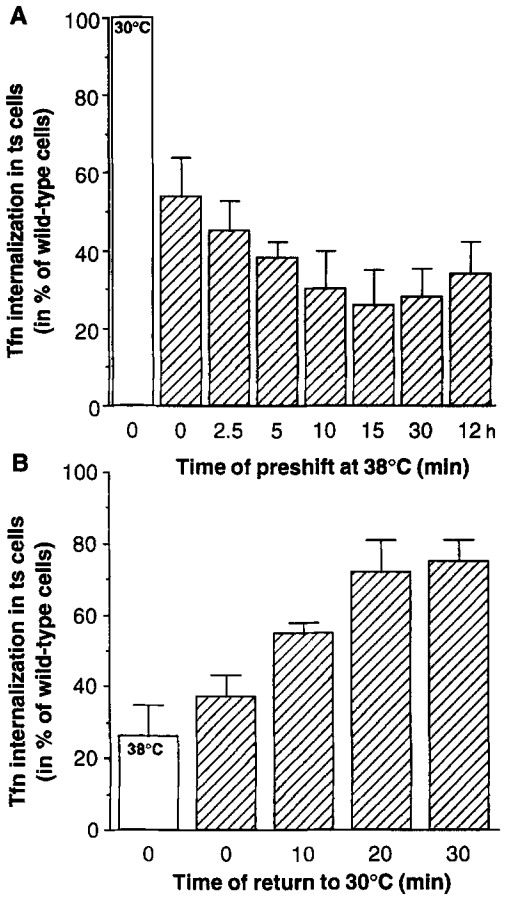

Figure 3. Kinetics for the onset of inhibition of endocytosis after temperature shift and of the recovery after return to the permissive temperature. (*A*) Cells expressing the dyn^{ts} mutant were preincubated for the indicated times at 38°C, BSST was added and its internalization was followed for 10 min at either 30°C (*open bar*) or 38°C (*striped bar*); n = 3. (*B*) Dyn^{ts} cells were preshifted for 15 min at 38°C and then returned to 30°C for the indicated times. BSST was added and its internalization was followed for 10 min at either 38°C (*open bar*) or 30°C (*striped bar*); n = 2. The results are expressed as the percentage of BSST endocytosis in dyn^{wt} cells assayed in parallel.

nonpermissive temperature and inhibition persisted even when cells were maintained for 12 h at 38°C (Fig. 3 *A*). These results suggest a direct role for mammalian dynamin in endocytic coated vesicle formation.

The temperature-sensitive inhibition of Tfn-internalization was reversible. Tfn internalization (Fig. 3 *B*) began to recover immediately after return to the permissive temperature and by 20 min, Tfn-internalization in dyn^{ts} mutants recovered to ~75% of wt cells assayed under identical conditions. The complementary immunofluorescence experiment in Fig. 4 shows that Texas Red-conjugated Tfn was efficiently internalized into cells expressing dyn^{wt} during a 10-min incubation and accumulated in the recycling endosomal compartment at both permissive and nonpermissive temperatures (Fig. 4, *a'* and *c'*, respectively). Similarly, internalization of Tfn at 30°C was normal in dyn^{ts} cells (compare *b'* with *a'*). In contrast, intracellular accumulation of Tfn was severely reduced when the dyn^{ts} cells were incubated at 38°C (compare Fig. 4, *d'* to *c'*). However, the ts-defect in endocytosis was rapidly reversed by returning the cells to 30°C for 10 min before addition of Tfn and further incubation at 30°C (Fig. 4 *e'*).

The immunofluorescence pattern for dyn^{wt} and dyn^{ts} at the permissive and nonpermissive temperatures is also shown in Fig. 4 (*a–e*). As previously described (van der Bliek et al., 1993; Damke et al., 1994), most of the overexpressed dynamin was cytosolic, suggesting that the membrane association of dynamin is saturable. Strikingly, at the nonpermissive temperature the dyn^{ts} mutant formed large aggregates in the cytoplasm (Fig. 4 *d*). These aggregates were reminiscent of those previously seen in cells expressing a 272-amino acid NH_2-terminal deletion mutant of dynamin lacking the GTPase domain (Herskovits et al., 1993). Aggregation was apparently reversible as the dynamin aggregates dispersed within 30 min after returning cells to the permissive temperature (Fig. 4 *e*).

The most striking morphological phenotype of dyn^{K44A} cells examined at longer times after induction was that cells became flat and spread radially (Damke et al., 1994). This was associated with rearrangements of the actin cytoskeleton from radial stress fibers to the cell periphery. Our earlier arguments that this was an indirect consequence of the block in endocytosis were confirmed using the dyn^{ts} cells since no such alterations were detected even after several hours at the nonpermissive temperature (not shown). Ultrastructural analysis of dyn^{ts} cells was performed using thin section electron microscopy. The amorphous structures of the dynamin aggregates formed after 15 min at the nonpermissive temperature are visible in Fig. 5 *A*. Preembedding and immunogold labeling confirmed that these large aggregates were heavily stained with the dynamin specific antibody, hudy-1 (not shown, but see Fig. 4 *d*). Curved coated pits accumulated at the cell surface of dyn^{ts} cells (see for example, Fig. 5 *B*). Quantitation of the number of cell surface coated pits was performed as described in Materials and Methods and revealed an approximately fourfold increase in the number of endocytic coated pits in dyn^{ts} cells held at the 38°C for 15 min (89 coated pits/mm cell surface; 982 μm counted) as compared to dyn^{wt} cells at 38°C (21 coated pits/mm cell surface; 516 μm counted). This accumulation was even greater than that observed at the surface of dyn^{k44A} mutant cells (Damke et al., 1994) and probably reflects the finding that the long membrane invaginations, often with coated ends, seen in dyn^{K44A} cells did not accumulate at early times in the dyn^{ts} cells (Fig. 5 *A*).

The Formation of Constricted Coated Pits Is Blocked in dyn^{ts} Cells

We have previously shown that expression of the dyn^{K44A} mutant defective in GTP binding and hydrolysis blocked endocytic coated vesicle formation at a stage after coated pit assembly and invagination but preceding the formation of constricted coated pits (Damke et al., 1994). Coated vesicle formation was blocked at a similar stage in dyn^{ts} cells. The sequestration of receptor-bound ligands, biotinylated via cleavable disulfide bonds, into constricted coated pits can be distinguished biochemically from their subsequent internalization into sealed coated vesicles (Schmid and Smythe, 1991; Carter et al., 1993). Ligands sequestered into constricted coated pits become inaccessible to avidin, but remain accessible to the small membrane impermeant reducing agent, MesNa (β-mercaptoethane sulfonic acid). The data in Fig. 6 show that sequestration and internalization are equally inhibited in dyn^{ts} cells indicating that the block in endocytosis precedes the formation of constricted coated pits. These results are consistent with the phenotype of *shibire* flies in which coated pits accumulating at the cell surface of nonneuronal cells remain accessible to large probes such as wheat germ agglutinin-conjugated HRP (Kosaka and Ikeda, 1983*a*).

Together, these results establish that the human dyn^{ts} mutant is functionally homologous to *Drosophila* $shibire^{ts1}$. Using this mutation, we have generated the first mammalian cell line with a rapid and reversible temperature-sensitive defect in receptor-mediated endocytosis.

Fluid Phase Endocytosis Is Only Partially Inhibited in dyn^{ts} Cells

We previously showed that nonselective pinocytosis of the fluid phase marker, HRP, continued in dyn^{K44A} cells at the same rates as in dyn^{wt} cells (Damke et al., 1994). Since clathrin-dependent endocytosis was severely inhibited we argued that a clathrin-independent pathway of pinocytosis may have been induced to compensate for the loss of the clathrin-dependent contribution to bulk pinocytosis. The rapid and selective temperature-sensitive inhibition of clathrin-dependent endocytosis in the dyn^{ts} cells has allowed us to confirm this hypothesis. The data in Fig. 7 *A* show that at the permissive temperature fluid phase endocytosis of HRP occurs with equal efficiency in dyn^{wt} and dyn^{ts} cells. In contrast to results obtained with the dyn^{K44A} cells, fluid phase endocytosis of HRP at the nonpermissive temperature was reduced by ~50% in dyn^{ts} cells compared to dyn^{wt} cells (Fig. 7 *B*). However, while Tfn-internalization in dyn^{ts} cells was potently inhibited at the nonpermissive temperature, substantial fluid phase uptake continued.

Importantly, at later times of incubation at the nonpermissive temperature, although clathrin-dependent Tfn endocytosis remained blocked, fluid phase endocytosis of HRP fully recovers. The data in Fig. 8 show that after a brief lag but within 30 min, fluid phase uptake recovers to wt levels. In fact, at 60 and 120 min after shift to the non-

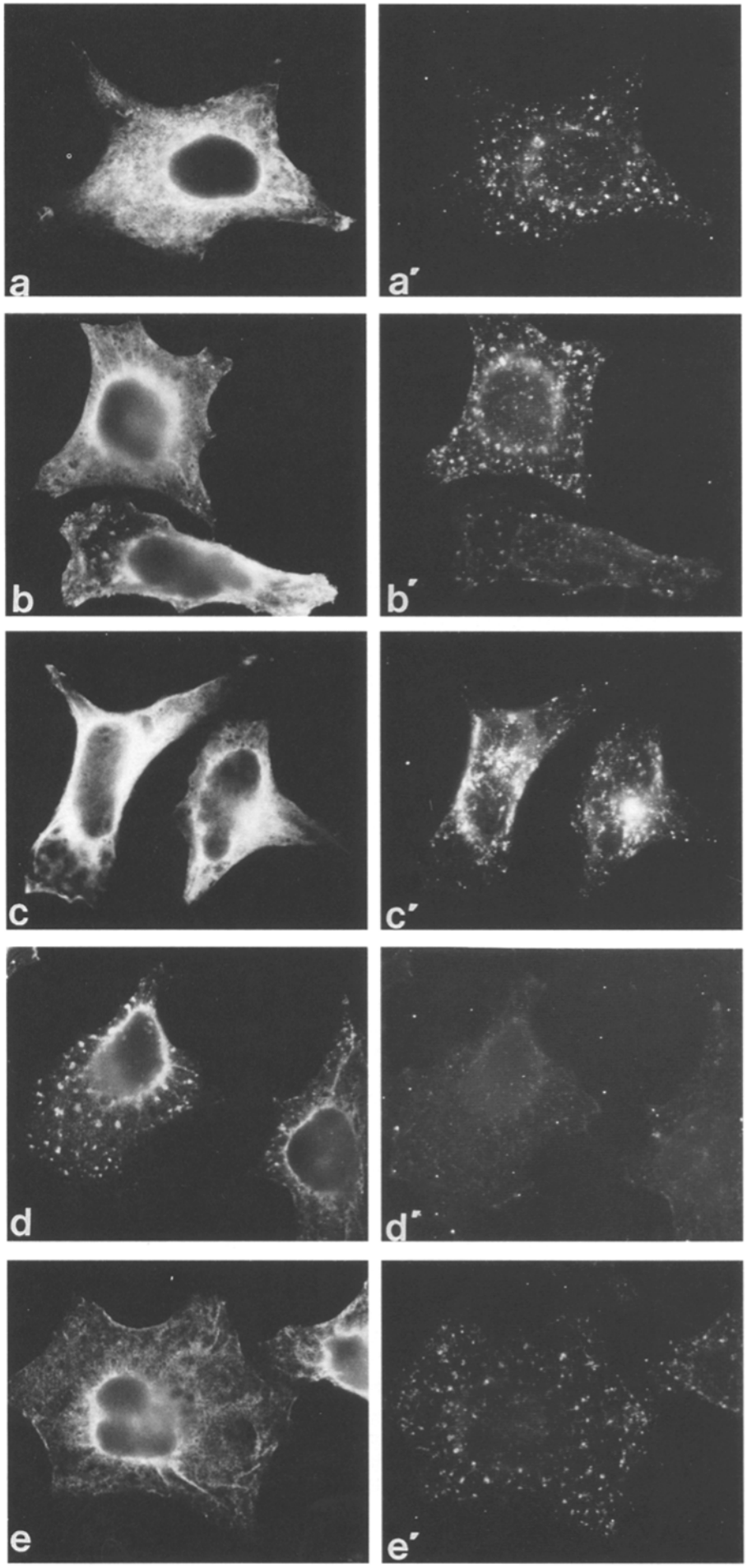

Figure 4. The immunofluorescence pattern for overexpressed dyn^{wt} (*a* and *c*) and dyn^{ts} (*b*, *d*, and *e*) detected with anti-HA antibody 12CA5 followed by a BODIPY FL-conjugated secondary antibody and for internalized Texas Red-conjugated transferrin (*a′–e′*). Cells were incubated at the permissive temperature (*a* and *b*; 30°C) or the nonpermissive temperature (*c* and *d*; 38°C) for 10 min with Texas Red-Tfn. Alternately, cells were preincubated at 38°C for 10 min, returned to 30°C for 30 min and then incubated with Texas Red-Tfn for 10 min at 30°C (*e*). At the nonpermissive temperature dynamin forms large aggregates in the cytosol (*d*) and cells do not internalize Tfn (*d′*). These aggregates were dispersed within 30 min when the cells are returned to the permissive temperature (*e*) and the ability of cells to internalize transferrin was restored (*e′*).

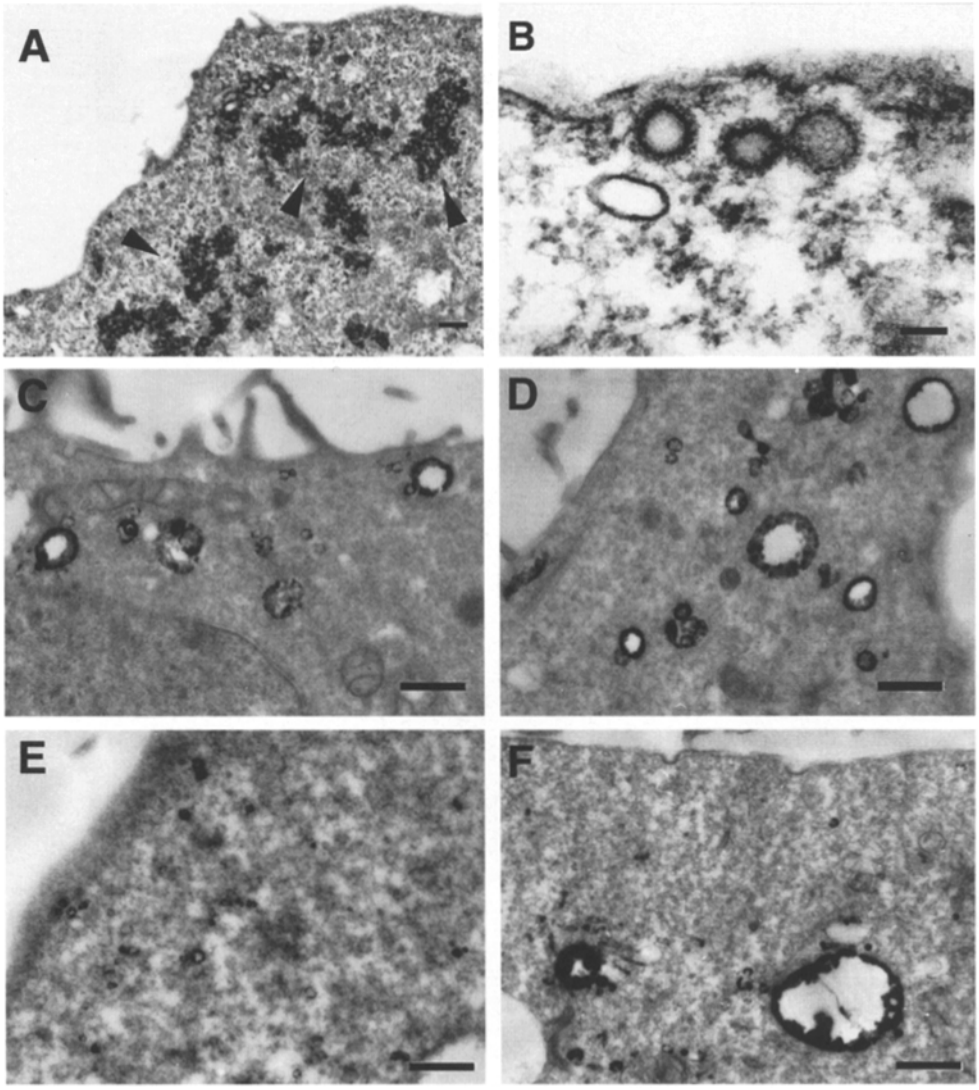

Figure 5. *A* and *B* show unlabeled thin-section electron micrographs of dyn^{ts} cells that had been incubated at 38°C for 15 min. Large aggregates that form in dyn^{ts} cells are clearly visible (*A*, *arrowheads*). Also seen are numerous coated pits that accumulate on the plasma membrane at the nonpermissive temperature, shown at higher magnification in *B* (*arrow*). (*C–F*) Electron micrographs showing ultrathin sections of the early endocytic compartments in wild-type (*C*) and dyn^{ts} mutant (*D–F*) cells. 72 h after induction at 32°C the cells were either incubated at 30° (*D*), at 38°C for 10 min (*C* and *E*) or at 38°C for 2 h (*F*). The media was replaced with serum free medium containing HRP (4 mg/ml) and the cells were further incubated at the same temperatures for 10 min. The tTA HeLa cells were washed and fixed in 2.5% glutaraldehyde in 0.1 M phosphate buffer, pH 7.4 for 30 min and incubated with 0.02% diaminobenzidine with 0.005% H_2O_2. After fixation with 2% OsO_4 for 30 min samples were embedded in Epon as described. Bar: (*A* and *C–F*) 500 nm; (*B*) 100 nm.

permissive temperature we observed a small but reproducible overcompensation to as much as 20% higher than wt levels. After 12 h of incubation at the nonpermissive temperature the rate of fluid phase endocytosis has been restored to wt levels. At this time point, Tfn internalization was still potently inhibited (see Fig. 3 *A*). This result was consistent with dyn^{K44A} cells that showed wt levels of fluid phase endocytosis 48 h after induction of dynamin expression (Damke et al., 1994). These results suggest that a constitutive clathrin-independent pathway for pinocytosis occurs in tTA-HeLa cells and confirm our earlier suggestion that this pathway is up-regulated in compensation for the loss of clathrin-dependent endocytosis.

A Clathrin-independent Mechanism for Pinocytosis in dyn^{ts} Cells

Several possible mechanisms of clathrin-independent pinocytosis have been described (reviewed by van Deurs et al., 1989; Watts and Marsh, 1992). These can be pharmacologically distinguished from clathrin-dependent endocytosis, which is selectively inhibited by K^+-depletion, cytosol acidification or hypertonicity (Larkin et al., 1983; Daukas and Zigmond, 1985; Sandvig et al., 1987). Cytosol acidification, one of the best characterized of these treatments, causes the accumulation of adherant coated pits at the plasma membrane (Heuser, 1989; Hansen et al., 1993) and effectively inhibits receptor-mediated endocytosis while bulk endocytic processes continue (Sandvig et al., 1987). Likewise, with dyn^{wt} cells, cytosol acidification severely (>85%) reduced receptor-mediated endocytosis of Tfn (Fig. 9 *A*) while fluid phase endocytosis of HRP was only partially (~50%) inhibited (Fig. 9 *B*). The acid-resistant component of HRP endocytosis corresponded quantitatively to the residual HRP uptake that occurred in dyn^{ts} cells at early times after shift to the nonpermissive temperature (Fig. 9 *B*, compare dyn^{wt} [*open bars*] with dyn^{ts} 15 min [*striped bars*]). Furthermore, the residual HRP uptake in dyn^{ts} cells was insensitive to cytosol acidification, consistent with the notion that it occurred via a clathrin-independent mechanism. Importantly, the residual Tfn uptake in dyn^{ts} cells was also resistant to cytosol acidification (Fig. 9 *A*), suggesting that it occurred through bulk pinocytic mechanisms and further strengthening our argument for a potent block in clathrin-dependent endocytosis in dyn^{ts} cells.

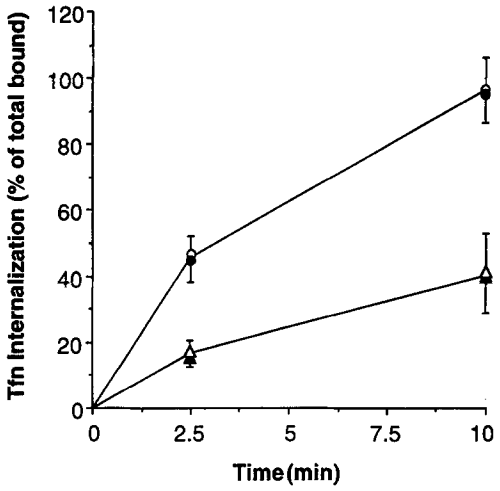

Figure 6. Expression of the dyn^{ts} mutant blocks BSST internalization preceding its sequestration into constricted coated pits. Cells expressing either wild-type (●, ○) or the dyn^{ts} mutant (▲, △) were harvested 72 h after induction at 32°C, preshifted for 10 min at 38°C, and incubated with BSST for the indicated times at 38°C. The extent of Tfn internalization was assessed by avidin inaccessibility (●, ▲) or MesNa-resistance (○, △) in four independent experiments as described in Materials and Methods.

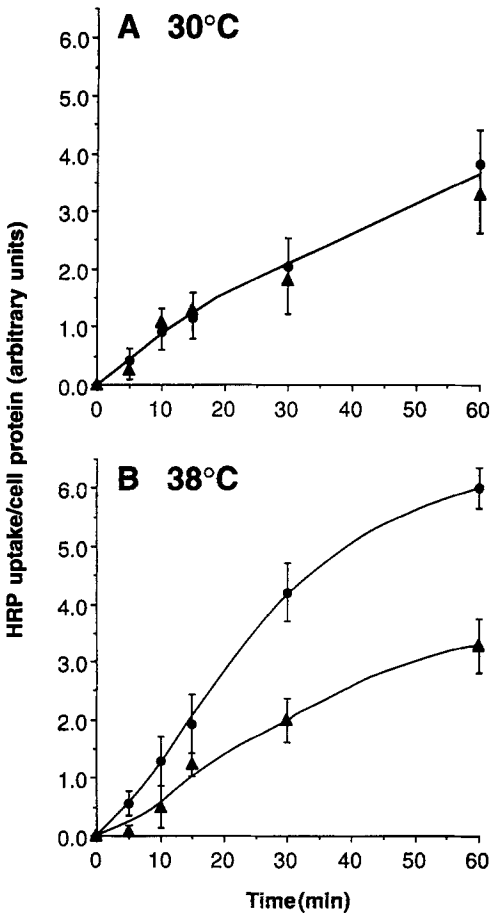

Figure 7. Fluid phase uptake in dyn^{ts} cells is partially inhibited after shift to the nonpermissive temperature. Cells expressing dyn^{wt} (●) and dyn^{ts} (▲) were incubated with 4 mg/ml HRP for up to 60 min at 30°C (*A*). In *B* the cells were preshifted to 38°C for 15 min and then incubated for the indicated times with HRP at 38°C. To ensure low backgrounds, cells were returned to ice and thoroughly washed before extracellular HRP was removed by digestion with 0.1% pronase for 10 min at 4°C. Cells were then pelleted through a sucrose cushion and lysed. Intracellular HRP was photometrically quantified after enzymatic reaction with *o*-phenylenediamine. The data of $n = 3$ (± SD) experiments are expressed relative to cell protein.

After a prolonged (120 min) incubation at the nonpermissive temperature fluid phase uptake in the dyn^{ts} cells had returned to near normal levels. This induced pinocytic pathway was now resistant to the effects of cytosol acidification (Fig. 9, compare dyn^{ts} 120 min, [*open* and *striped bars*]). Again, Tfn uptake at this time point remained severely inhibited. Cells expressing the constitutively defective dyn^{K44A} mutant provide an additional control for long-term incubations in the absence of functional dynamin. As for the dyn^{ts} cells, both the residual Tfn uptake and the induced HRP uptake in these cells were resistant to the inhibitory effects of cytosol acidification (Fig. 9, *A* and *B*). To rule out effects on endosomal trafficking that might lead to reduced accumulation of HRP (Cupers et al., 1994), the data in Fig. 9 were derived from an early time point after HRP uptake (15 min) before the inflection in the initial rate of uptake occurred (see Fig. 7). In addition, to ensure that cytosol acidification effects were related to internalization and not recycling, the rates of efflux (regurgitation) of HRP in the dyn^{ts} mutant cells were measured directly and found to be unaffected (not shown). This is consistent with our previous finding that Tfn recycling was unaffected in dyn^{K44A} cells. These results confirm that the compensation in bulk endocytosis was mediated by an acid-resistant pinocytic process mechanistically distinct from clathrin-mediated endocytosis.

The effect of other pharmacological treatments on the clathrin-independent pathway induced in dyn^{ts} cells were examined to further characterize this pathway. Specifically we examined the effects of cytochalasin D, which has been shown to selectively inhibit endocytosis at the apical membrane of polarized epithelial cells (Gottlieb et al., 1993) and to inhibit the internalization of caveolae-associated proteins in some cells (Parton et al., 1994) and hexamethylamiloride, which has been shown to selectively inhibit macropinocytosis (West et al., 1989; Hewlett et al., 1994). Neither the residual HRP uptake at early times after shift to the nonpermissive temperature nor the induced uptake occurring after prolonged incubations were affected by these treatments (data not shown).

Since there was significant residual fluid phase uptake in dyn^{ts} cells, HRP was used as a probe to compare the ultrastructure of the early endocytic pathway at permissive and nonpermissive temperatures. 10 min after incubating wild-type cells at 38°C with HRP, most of the electron-dense DAB reaction product could be detected in large heterogeneously shaped endosomal vesicles (100–600-nm diam) and thin tubules (Fig. 5 *C*). A similar distribution of internalized HRP was seen in dyn^{ts} cells when incubated at the permissive temperature of 30°C (Fig. 5 *D*). In contrast, when the dyn^{ts} cells were incubated at 38°C for 10 min, HRP labeling was predominantly detected in a small (<70-nm diam) and more homogeneous population of vesicles

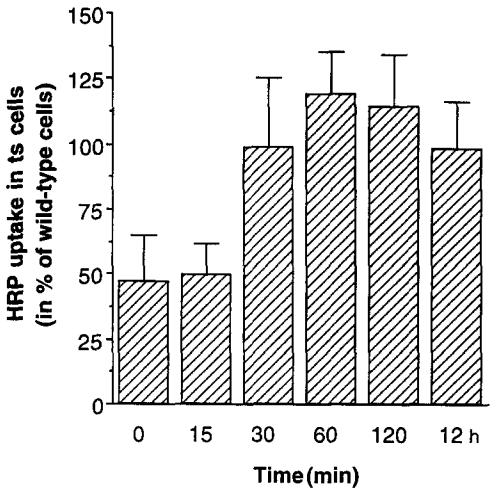

Figure 8. Recovery of fluid phase endocytosis in dyn^{ts} cells after shift to the nonpermissive temperature. Dyn^{wt} and dyn^{ts} cells were grown on 35-mm dishes for 72 h at 32°C in the absence of tetracycline. After incubation at the nonpermissive temperature for the indicated times, fluid phase uptake of HRP (4 mg/ml) was followed for 15 min at 38°C. Cells were rapidly cooled by repeated washes on ice and samples were processed as described in Materials and Methods (n = 3).

(Fig. 5 *E*). Together with the acid-resistant properties of HRP uptake in the dyn^{ts} cells, these results were most consistent with a role for the noncoated vesicles described by Sandvig, van Deurs, and colleagues (Hansen et al., 1993; Sandvig and van Deurs, 1994) in compensating for the loss of clathrin-dependent endocytosis.

Interestingly, larger endosomal structures were not readily detectable after HRP uptake in dyn^{ts} cells at early times after shift to the nonpermissive temperature (Fig. 5 *C*). However, after prolonged incubation (120 min) at the nonpermissive temperature, when the bulk rate of endocytosis had recovered to wt levels, large endosomal compartments could again be labeled after a 10-min incubation with HRP (Fig. 5 *F*). These data strongly suggest that the early endosomal compartment rapidly contracts (within 10 min) and later expands in response to the magnitude of incoming endocytic membrane. Although quantitative morphometric analyses will be necessary to confirm this hypothesis, similar observations have been made in studies on *shibire* (Kessell et al., 1989; Koenig and Ikeda, 1990).

Discussion

We have generated a mammalian cell line with a specific and molecularly defined temperature-sensitive defect in receptor-mediated endocytosis. These cells overexpress a human dynamin mutant (G273D) that is homologous to the $shibire^{ts1}$ allele in *Drosophila*. In many ways, the phenotype of these cells resembles that of *shibire* flies. Receptor-mediated endocytosis occurs at wild-type rates at the permissive temperature of 30°C but is severely inhibited at the nonpermissive temperature of 38°C. The ts phenotype shows rapid onset and is reversible upon return to the permissive temperature. Invaginated, but not constricted, coated pits accumulate on the cytoplasmic surface of the

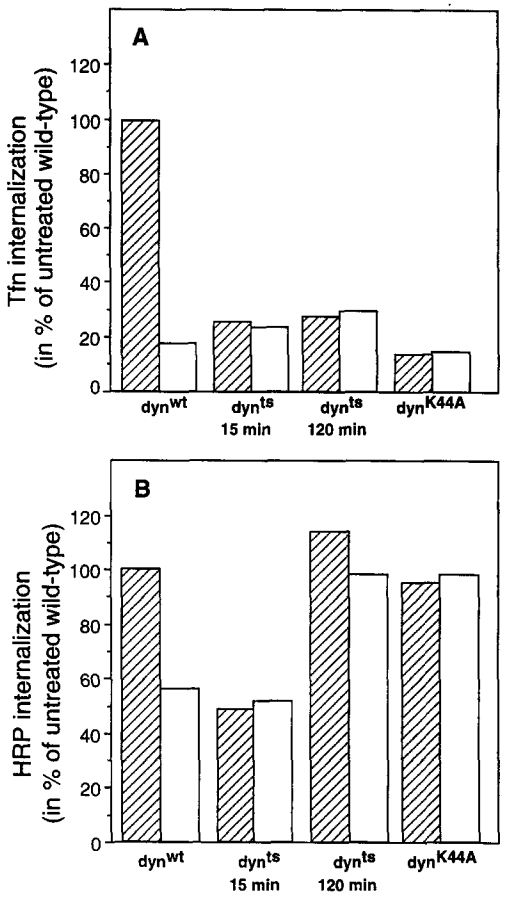

Figure 9. Effect of cytosol acidification on Tfn (*A*) and HRP (*B*) internalization in induced dyn^{wt}, dyn^{ts}, and dyn^{K44A} cells. The dyn^{ts} cells were preshifted to 38°C for either 15 min or 2 h as indicated. Cells were treated with 10 mM acetic acid, pH 5.0 (*open bars*) or left untreated (*striped bars*) during the last 15 min (i.e., during the preshift) before internalization assays were performed. For details see Materials and Methods. Shown are the averaged results from two independent experiments performed in duplicate.

plasma membranes. Like the previously characterized HeLa cell line expressing the dyn^{K44A} mutant defective in GTP binding and hydrolysis, the dyn^{ts} cells exhibit a specific defect in endocytic clathrin-coated vesicle formation.

Dynamin Functions as an Oligomer in Coated Vesicle Budding

Previous genetic analysis of *shibire* heterozygotes had suggested that the *shibire* gene product acts as a multimeric protein (Kim and Wu, 1990). Our finding, that purified dynamin exists as a tetramer that spontaneously self-assembles in vitro into rings and helical stacks of rings (Hinshaw and Schmid, 1995), confirms this hypothesis. The dynamin rings formed in vitro are identical in dimension to "collars" originally observed around the necks of the membrane invaginations that accumulated at nerve terminals in *shibire* flies incubated at the nonpermissive temperature (Kosaka and Ikeda, 1983*b*; Koenig and Ikeda, 1989). More recently, when permeabilized synaptic terminals isolated from rat brain were incubated with GTPγS, the nonhydrolyzable analogue of GTP, bands of dynamin were ob-

served encircling the elongated necks of coated pits that accumulated (Takei et al., 1995). Thus, in both *shibire*^{ts} and GTPγS-treated nerve termini, dynamin apparently accumulates in ring structures at the necks of invaginated coated pits clearly segregated from the clathrin lattice at their base. This distribution contrasts with the immunolocalization of the dyn^{K44A} mutant that is uniformly distributed throughout the clathrin lattices of flat and curved coated pits (Damke et al., 1994). These results suggested a model (Hinshaw and Schmid, 1995) in which dynamin, in its unoccupied or GDP-bound form, is first recruited to and uniformly distributed on flat or curved clathrin lattices. Subsequent GTP-GDP exchange would result in a conformational change that alters dynamin-dynamin interactions or interactions between dynamin and some, as yet unidentified, targeting and/or assembly molecule. GTP-bound dynamin is redistributed to the necks of invaginated pits and assembles into collars, resulting in the formation of constricted coated pits. Since the dyn^{K44A} has reduced affinity for GTP, this step is blocked (Damke et al., 1994). Conversely, in the presence of a nonhydrolyzable analogue of GTP, these structures become exaggerated (Takei et al., 1995). We have proposed that GTP hydrolysis would result in a second concerted conformation change of the dynamin collars to drive vesicle budding (Hinshaw and Schmid, 1995).

A Model for the Defect in dyn^{ts} Cells

How might the dyn^{ts} phenotype be explained in the context of this working model for dynamin function? First, our model predicts that dynamin functions as a large homo-oligomer involving the concerted action of multiple dynamin polypeptides (Hinshaw and Schmid, 1995). This would explain how expression of the dyn^{ts} mutant in the presence of endogenous wild-type dynamin gives a ts-phenotype. At the levels of overexpression achieved (>20-fold) each functional oligomer would contain very few wt dynamin polypeptides, thus the dyn^{ts} phenotype would be dominant.

Interestingly, when synthesized at 37°C the dyn^{ts} phenotype is silent and there is no apparent interference with the function of wt-dynamin. This suggests that dyn^{ts} is misfolded under these conditions so that it cannot interact with endogenous dynamin. An important consequence of this observation is that during long-term incubation at 38°C, newly synthesized dyn^{ts} would be nonfunctional and the mutant hetero-oligomers would be gradually replaced with wt dynamin homo-oligomers. This could explain why phenotypes seen at longer incubation times with the dyn^{K44A} mutant, such as alterations in the actin cytoskeleton, are not observed in dyn^{ts} cells.

The mutation that generates the ts phenotype (G273D) exchanges a flexible glycine residue for a less flexible aspartic acid residue at the boundary between the GTPase domain and the COOH-terminal two-thirds of dynamin. When overexpressed in HeLa cells, the dyn^{ts} mutant, like the dyn^{K44A} mutant, blocks the formation of constricted coated pits, suggesting that it is also defective in GTP binding. In contrast, collared and, according to our model, constricted coated pits accumulate at the nerve termini of *Drosophila* expressing the analogous mutant (Kosaka and Ikeda, 1983*b*), suggesting that the *shibire*^{ts1} gene product might be defective in GTP hydrolysis. However, the conserved GTP binding elements in dynamin are unchanged by this mutation so that neither GTP binding nor hydrolysis are likely to be affected by the dyn^{ts} mutation. Instead, we speculate that the COOH-terminal two-thirds of dynamin is uncoupled from the NH_2-terminal GTPase domain by this mutation. Interestingly, the aggregate formed by dyn^{ts} at the nonpermissive temperature are similar to those formed by a mutant dynamin lacking the entire GTPase domain (Herskovits et al., 1993). Large-scale expression of recombinant dyn^{ts} mutant is being performed to directly test this hypothesis.

The suggestion that the dyn^{ts} mutant is defective in transmitting conformational information from its NH_2-terminal GTPase domain to its COOH-terminal domains would reconcile the apparent phenotypic differences between dyn^{ts} HeLa cells and *shibire* neurons. Such a defect would block both the conversion of dynamin-GDP to dynamin-GTP (preventing the formation of constricted coated pits, as in the dyn^{K44A} mutant), and the conversion of dynamin-GTP to dynamin-GDP (leading to the accumulation of collars, as seen in GTPγS treated neurons). The phenotype observed would depend on the stage in its GTP cycle predominantly occupied by dynamin before the temperature shift. Interestingly, as in HeLa cells, collared pits were not observed in non-neuronal tissues of *shibire* flies (Kosaka and Ikeda, 1983*a*). Therefore it is possible that in neurons, dynamin might be specifically held at a late stage, in its GTP-bound form, to facilitate rapid endocytosis after depolarization. The selective regulation of neuronal dynamin-1 by phosphorylation/dephosphorylation (Robinson et al., 1993) might be involved in triggering dynamin function for rapid synaptic vesicle recycling (Morris and Schmid, 1995).

Dynamin and Clathrin-independent Pinocytosis

Apparently unlike the *shibire* phenotype, fluid phase endocytosis continues at the nonpermissive temperature in HeLa cells expressing the dyn^{ts} mutant. At early times after shift to the nonpermissive temperature, fluid phase endocytosis is partially inhibited reflecting the contribution of clathrin-mediated endocytosis to overall pinocytosis in HeLa cells. Strikingly, after prolonged incubation at the nonpermissive temperature fluid phase uptake increases to fully compensate for the loss of clathrin-dependent endocytosis. Studies on fluid phase uptake in *shibire* flies have been limited to early times after shift to the nonpermissive temperature. Therefore it is possible that a compensatory pathway would also be induced in *shibire* cells after prolonged incubation. It is also possible that the relative contributions of clathrin-dependent and clathrin-independent pinocytosis varies between cell types as it does in different organisms. Clathrin deficient yeast, for example, show only a partial reduction in endocytosis (Payne et al., 1988) whereas fluid phase uptake is inhibited by ~80% in clathrin-deficient *Dictyostelium* (Ruscetti et al., 1994).

The rapid block in clathrin-mediated endocytosis in dyn^{ts} cells has revealed the existence of a constitutive clathrin-independent mechanism for endocytosis in HeLa cells. A number of studies have established that fluid

phase pinocytosis can continue under conditions where receptor-mediated uptake is severely inhibited (Daukas and Zigmond, 1985; Moya et al., 1985; Sandvig et al., 1987). Morphological studies have identified smooth endocytic vesicles as mediators of these clathrin-independent endocytic events (Huet et al., 1980; Hansen et al., 1991). However, these studies have largely relied on the use of treatments with poorly understood mechanisms of inhibition of clathrin-dependent endocytosis, namely K^+-depletion, cytosol acidification and hypertonicity. These treatments have variable effects on different cell types and are not always selective (reviewed by van Deurs et al., 1989). Others have argued that the rate of clathrin-dependent endocytosis can account for total fluid phase uptake (Marsh and Helenius, 1980; Griffiths et al., 1989; Pelchen-Matthews et al., 1991) and that clathrin-independent pathways might only be induced in response to the nonphysiological conditions required to inhibit clathrin-dependent endocytosis (Watts and Marsh, 1992; Cupers et al., 1994). As a result the significance and even the existence of a constitutive clathrin-independent pathway for endocytosis has been questioned (Watts and Marsh, 1992).

The results presented here provide strong evidence for a constitutive clathrin and dynamin-independent pathway for pinocytosis in HeLa cells and further suggest that this pathway can be up-regulated to compensate for the loss of clathrin-dependent endocytosis. In dyn^{wt} cells, Tfn uptake is severely inhibited by cytosol acidification while HRP uptake is partially inhibited. Importantly, the residual uptake of both Tfn and HRP that occurs in dyn^{ts} cells early after shift to the nonpermissive temperature and the induced uptake of HRP that occurs at later times after shift to the nonpermissive temperature are resistant to cytosol acidification. Thus the pinocytosis that occurs in dyn^{ts} cells can be mechanistically distinguished from clathrin-dependent endocytosis. Induction of bulk-phase endocytosis to fully compensate for inhibition of clathrin-mediated endocytosis was recently observed in rat fetal fibroblasts after K^+-depletion or incubation in hypertonic media (Cupers et al., 1994). Based on our results, the 30-min incubations required for these inhibitory effects would suffice for induction of an alternate pinocytic pathway.

Interestingly, yeast cells expressing a temperature-sensitive defect in a clathrin-mediated pathway also induce a compensatory clathrin-independent pathway when maintained at the nonpermissive temperature. At early times after shift to the nonpermissive temperature, chc-ts1 yeast cells carrying a temperature-sensitive clathrin mutant show a strong defect in sorting of vacuolar enzymes. However, the chc-ts1 cells regain the ability to efficiently sort vacuolar enzymes when maintained at the nonpermissive temperature for 3 h (Seeger and Payne, 1992). The nature of this compensatory pathway for efficient vacuolar enzyme sorting in yeast is also unknown.

After prolonged incubation at the nonpermissive temperature HRP uptake increases approximately twofold recovering to wt levels. In contrast, the residual Tfn uptake is not apparently increased. Some of this residual Tfn uptake may occur due to an incomplete block in coated vesicle formation. Alternatively, it is possible that Tfn-R are not freely mobile in the membrane, perhaps trapped in coated pits, and are therefore not a reliable bulk membrane marker. By geometric considerations, we would expect that Tfn-uptake would be increased less significantly than HRP uptake. HRP uptake would increase proportionally to volume, whereas Tfn uptake would increase proportionally to surface area. Further studies will be needed to resolve the mechanism(s) of pinocytosis in cells expressing mutant dynamin.

The data presented here, together with our previous characterization of dyn^{K44A} cells and the specific localization of endogenous and overexpressed dynamin molecules to clathrin coated pits on the plasma membrane (Damke et al., 1994), suggest that overexpression of these dynamin mutants potently and selectively inhibits clathrin-mediated endocytosis. In addition to providing a valuable new tool for the functional and mechanistic analysis of clathrin-independent pinocytic pathways, the properties of these cells make them ideal for addressing a variety of important issues in cell biology. These include, how specific receptor-ligand complexes or pathogens enter cells, whether a protein is transiently expressed on the cell surface en route to another intracellular location and the role of receptor-mediated endocytosis in such processes as cell adhesion, cell motility and signal transduction.

We thank our colleagues in the Schmid lab for helpful discussions and for comments on the manuscript. Dr. C.-M. Chang assisted in electron microscopy.

This work was supported by National Institutes of Health grant GM42445 to S. L. Schmid and a Muscular Dystrophy Association grant to A. M. van der Blick. S. L. Schmid is an Established Investigator of the American Heart Association. H. Damke was supported by fellowships from the Deutsche Forschungsgemeinschaft and the Muscular Dystrophy Association.

Received for publication 9 June 1995 and in revised form 19 July 1995.

References

Burnette, W. N. 1981. Western blotting: electrophoretic transfer of proteins from sodium dodecyl sulfate-polyacrylamide gels to unmodified nitrocellulose and radiographic detection with antibody and radioiodinated protein A. *Anal. Biochem.* 112:195–203.

Carter, L. L., T. E. Redelmeier, L. A. Woollenweber, and S. L. Schmid. 1993. Multiple GTP-binding proteins participate in clathrin-coated vesicle-mediated endocytosis. *J. Cell Biol.* 120:37–45.

Chen, M. S., R. A. Obar, C. C. Schroeder, T. W. Austin, C. A. Poodry, S. C. Wadsworth, and R. B. Vallee. 1991. Multiple forms of dynamin are encoded by *Shibire*, a *Drosophila* gene involved in endocytosis. *Nature (Lond.).* 351: 583–586.

Cook, T. A., R. Urrutia, and M. A. McNiven. 1994. Identification of dynamin 2, an isoform ubiquitously expressed in rat tissues. *Proc. Natl. Acad. Sci. USA.* 91:644–648.

Cupers, P., A. Veithen, A. Kiss, P. Baudhin, and P. J. Courtoy. 1994. Clathrin polymerization is not required for bulk-phase endocytosis in rat fetal fibroblasts. *J. Cell Biol.* 127:725–735.

Damke, H., T. Baba, D. E. Warnock, and S. L. Schmid. 1994. Induction of mutant dynamin specifically blocks endocytic vesicle formation. *J. Cell Biol.* 127:915–934.

Damke, H., M. Gossen, S. Freundlieb, H. Bujard, and S. L. Schmid. 1995. Tightly regulated and inducible expression of a dominant interfering dynamin mutant in stably transformed HeLa cells. *Methods Enzymol.* 257:209–220.

Daukas, G., and S. H. Zigmond. 1985. Inhibition of receptor mediated but not fluid phase endocytosis in polymorphonuclear leukocytes. *J. Cell Biol.* 101: 1673–1679.

Gossen, M., and H. Bujard. 1992. Tight control of gene expression in mammalian cells by tetracycline-responsive promoters. *Proc. Natl. Acad. Sci. USA.* 89:5547–5551.

Gottlieb, T. A., I. E. Ivanov, M. Adesnik, and D. D. Sabatini. 1993. Actin microfilaments play a critical role in endocytosis at the apical not the basolateral surface of polarized epithelial cells. *J. Cell Biol.* 120:695–710.

Griffiths, G., R. Back, and M. Marsh. 1989. A quantitative analysis of the endocytic pathway in baby hamster kidney cells. *J. Cell Biol.* 109:2703–2720.

Hansen, S. H., K. Sandvig, and B. van Deurs. 1991. The preendosomal compart-

ment comprises distinct coated and noncoated endocytic populations. *J. Cell Biol.* 113:731–741.

Hansen, S. H., K. Sandvig, and B. van Deurs. 1993. Clathrin and HA2 adaptors: effects of potassium depletion, hypertonic medium, and cytosol acidification. *J. Cell Biol.* 121:61–72.

Herskovits, J. S., C. C. Burgess, R. A. Obar, and R. B. Vallee. 1993. Effects of mutant rat dynamin on endocytosis. *J. Cell Biol.* 122:565–578.

Heuser, J. 1989. Effects of cytoplasmic acidification on clathrin lattice morphology. *J. Cell Biol.* 108:401–411.

Hewlett, L. J., A. R. Prescott, and C. Watts. 1994. The coated pit and macropinocytic pathways serve distinct endosome populations. *J. Cell Biol.* 124:689–703.

Hinshaw, J. E., and S. L. Schmid. 1995. Dynamin self-assembles into rings suggesting a mechanism for coated vesicle budding. *Nature (Lond.).* 374:190–192.

Huet, C., J. F. Ash, and S. J. Singer. 1980. The antibody-induced clustering and endocytosis of HLA antigens on cultured human fibroblasts. *Cell.* 21:429–438.

Kessell, I., B. D. Holst, and T. F. Roth. 1989. Membrane intermediates in endocytosis are labile, as shown in a temperature-sensitive mutant. *Proc. Natl. Acad. Sci. USA.* 86:4968–4972.

Kim. Y.-T., and C.-F. Wu. 1990. Allelic interactions at the *shibire* locus of *Drosophila*: effects on behaviour. *J. Neurogenet.* 7:1–14.

Koenig, J. H., and K. Ikeda. 1990. Transformational process of the endosomal compartment in nephrocytes of *Drosophila melanogaster. Cell Tissue Res.* 262:233–244.

Kosaka, T., and K. Ikeda. 1983*a*. Reversible blockage of membrane retrieval and endocytosis in the garland cell of the temperature-sensitive mutant of *Drosophila melanogaster, shibire*^{ts1}. *J. Cell Biol.* 97:499–507.

Kosaka, T., and K. Ikeda. 1983*b*. Possible temperature-dependent blockage of synaptic vesicle recycling induced by a single gene mutation in *Drosophila. J. Neurobiol.* 14:207–225.

Larkin, J. M., M. S. Brown, J. L. Goldstein, and R. G. W. Anderson. 1983. Depletion of intracellular potassium arrests coated pit formation and receptor-mediated endocytosis in fibroblasts. *Cell.* 33: 273–285.

Marsh, M., and A. Helenius. 1980. Adsorptive endocytosis of semliki forest virus. *J. Mol. Biol.* 142:439–454.

Marsh, M., S. L. Schmid, H. Kern, E. Harms, P. Male, I. Mellman, and A. Helenius. 1987. Rapid analytical and preparative isolation of functional endosomes by free flow electrophoresis. *J. Cell Biol.* 104:875–886.

Morris, S. A., and S. L. Schmid. 1995. Synaptic vesicle recycling: the Ferrari of endocytosis? *Curr. Biol.* 5:113–115.

Moya, M., A. Dautry-Varsat, B. Goud, D. Louvard, and P. Bouquet. 1985. Inhibition of coated pit formation in Hep_2 cells blocks the cytotoxicity of diphtheria toxin but not that of ricin toxin. *J. Cell Biol.* 101:548–559.

Nakata, T., A. Iwamoto, Y. Noda, R. Takemura, H. Yoshikura, and N. Hirokawa. 1991. Predominant and developmentally regulated expression of dynamin in neurons. *Neuron.* 7:461–469.

Nakata, T., R. Takemura, and N. Hirokawa. 1993. A novel member of the dynamin family of GTP-binding proteins is expressed specifically in the testis. *J. Cell Sci.* 105:1–5.

Parton, R. G., B. Joggerst, and K. Simons. 1994. Regulated internalization of caveolae. *J. Cell Biol.* 127:1199–1215.

Payne, G.S., D. Baker, E. van Tuinen, and R. Schekman. 1988. Protein transport to the vacuole and receptor-mediated endocytosis by clathrin heavy chain-deficient yeast. *J. Cell Biol.* 106:1453–1461.

Pelchen-Matthews, A., J. E. Armes, G. Griffiths, and M. Marsh. 1991. Differential endocytosis of CD4 in lymphocytic and non-lymphocytic cells. *J. Exp. Med.* 173:575–587.

Poodry, C. A., and L. Edgar. 1979. Reversible alterations in the neuromuscular junctions of *drosophila melanogaster* bearing a temperature-sensitive mutation, *shibire. J. Cell Biol.* 81:520–527.

Robinson, P. J., J.-M., Sontag, J.-P. Liu, E. M. Fykse, C. Slaughter, H. McMahon, and T. C. Südhof. 1993. Dynamin GTPase regulated by protein kinase C phosphorylation in nerve terminals. *Nature (Lond.).* 365:163-166.

Ruscetti, T., J. A. Cardelli, M. L. Niswonger, and T. J. O'Halloran. 1994. Clathrin heavy chain functions in sorting and secretion of lysosomal enzymes in *Dictyostelium. J. Cell Biol.* 126:343–352.

Sandvig, K., and B. van Deurs. 1994. Endocytosis and intracellular sorting of ricin and Shiga toxin. *FEBS Lett.* 346:99–102.

Sandvig, K., S. Olsnes, O. W. Petersen, and B. van Deurs. 1987. Acidification of the cytosol inhibits endocytosis from coated pits. *J. Cell Biol.* 105:679–689.

Schmid, S. L., and E. Smythe. 1991. Stage-specific assays for coated pit formation and coated vesicle budding in vitro. *J. Cell Biol.* 114:869–880.

Seeger, M., and G. S. Payne. 1992. A role for clathrin in the sorting of vacuolar proteins in the Golgi complex of yeast. *EMBO J.* 11:2811–2818.

Shpetner, H. S., and R. B. Vallee. 1989. Identification of dynamin, a novel mechanochemical enzyme that mediates interactions between microtubules. *Cell.* 59:421–432.

Smythe, E., T. E. Redelmeier, and S. L. Schmid. 1992. Receptor-mediated endocytosis in semi-intact cells. *Method Enzymol.* 219:223–234.

Sontag, J.-M., E. M. Fykse, Y. Ushkaryov, J.-P. Liu, P. J. Robinson, and T. C. Südhof. 1994. Differential expression and regulation of multiple dynamins. *J. Biol. Chem.* 269:4547–4554.

Takei, K., P. McPherson, S. L. Schmid, and P. De Camilli. 1995. Tubular membrane invaginations coated by dynamin rings are induced by GTPγS in nerve terminals. *Nature (Lond.).* 374:186–190.

Tsuruhara, T., J. H. Koenig, and K. Ikeda. 1990. Synchronized endocytosis studied in the oocyte of a temperature-sensitive mutant of *Drosophila melanogaster. Cell Tissue Res.* 259:199–207.

van der Bliek, A. M., and E. M. Meyerowitz. 1991. Dynamin-like protein encoded by the *Drosophila shibire* gene associated with vesicular traffic. *Nature (Lond.).* 351:411–414.

van der Bliek, A. M., T. E. Redelmeier, H. Damke, E. J. Tisdale, E. M. Meyerowitz, and S. L. Schmid. 1993. Mutations in human dynamin block an intermediate stage in coated vesicle formation. *J. Cell Biol.* 122:553–563.

van Deurs, B., O. W. Petersen, S. Olsnes, and K. Sandvig. 1989. The ways of endocytosis. *Int. Rev. Cytol.* 117:131–177.

Warnock, D. E., L. J. Terlecky, and S. L. Schmid. 1995. Dynamin GTPase is stimulated by crosslinking through the C-terminal proline-rich domain. *EMBO J.* 14:1322–1328.

Watts. C., and M. Marsh. 1992. Endocytosis: what goes in and how? *J. Cell Sci.* 103:1–8.

West, M. A., M. S. Bretscher, and C. Watts. 1989. Distinct endocytotic pathways in EGF stimulated human carcinoma A431 cells. *J. Cell Biol.* 109:2731–2739.